ERJ open research
THE BEST IN OPEN ACCESS BASIC, TRANSLATIONAL & CLINICAL RESPIRATORY RESEARCH

Early View

Original Research Article

Ciliated Epithelial Cell Differentiation at Air-Liquid Interface and RSV infection using Animal-Free Media and Substrates

Machaela Palor, Elizabeth K. Haughey, Jenny Herbert, Christopher O'Callaghan, Rosalind L. Smyth, Paolo De Coppi, Robert E. Hynds, Claire M. Smith

Please cite this article as: Palor M, Haughey EK, Herbert J, *et al*. Ciliated Epithelial Cell Differentiation at Air-Liquid Interface and RSV infection using Animal-Free Media and Substrates. *ERJ Open Res* 2025; in press (https://doi.org/10.1183/23120541.00028-2025).

Ciliated Epithelial Cell Differentiation at Air-Liquid Interface and RSV infection using Animal-Free Media and Substrates

Authors: Machaela Palor[1], Elizabeth K. Haughey[1], Jenny Herbert[2], Christopher O'Callaghan[1], Rosalind L. Smyth[1], Paolo De Coppi[1], Robert E. Hynds[3], Claire M. Smith[1*]

Affiliations

1. Infection, Immunity and Inflammation, UCL Great Ormond Street Institute of Child Health, University College London, London, UK.
2. School of Medical Sciences, Faculty of Biology, Medicine and Health, University of Manchester, UK
3. Epithelial Cell Biology in ENT Research (EpiCENTR) Group, Great Ormond Street UCL Institute of Child Health, University College London, London, UK

* Corresponding author:

Dr Claire Mary Smith,

UCL Great Ormond Street Institute of Child Health,

30 Guilford St, London WC1N 1EH,

c.m.smith@ucl.ac.uk

Abstract

Animal-derived components in cell culture, such as foetal bovine serum (FBS) and extracellular matrix proteins (ECM), pose ethical concerns and contribute to variability in experimental outcomes. This study explores the use of animal-free cell culture media and substrates to support the growth and differentiation of primary human bronchial epithelial cells (BECs), as well as their infection by respiratory syncytial virus (RSV).

We evaluated the performance of jellyfish collagen 0 and recombinant ECM proteins as alternatives to traditional mammalian substrates. Additionally, we assessed the use of animal-free media and human serum (HS) in viral propagation using HEp2 cells.

Results demonstrate that the use of animal-free medium and matrix proteins and human serum can support primary epithelial cell growth and differentiation, with high-levels of ciliation and barrier integrity. RSV propagation in animal-free medium produced an increase in viral titres, indicating the potential of these systems for anti-viral research.

Transitioning to include more animal-free medium and substrates for primary cell culture and viral propagation will help improve the ethical standing of research and offer more human-relevant models for studying viral diseases in the future.

Introduction

Cell culture systems are essential for studying cellular processes and viral infections. Traditionally, these systems use animal-derived products like foetal bovine serum (FBS) and collagen to provide nutrients and support for cell growth. However, these components raise ethical concerns, and introduce variability, as well as potential contamination risks (1). The need for animal-free alternatives is evident, aiming to reduce reliance on animal products while enhancing experimental reproducibility.

In December 2022, the U.S. enacted the FDA Modernization Act 2.0, allowing alternatives to animal testing—such as cell-based assays, organoids, and computational models—to play a more prominent role in the drug approval process. This change in legislation is accelerating the transition to animal-free research methodologies, including those that do not involve the use of animals or animal-derived products (2, 3). In cell culture, animal-free conditions—those completely devoid of animal-derived components—are thought to be important for enhancing assay reproducibility and regulatory compliance, especially in the context of producing cell-based therapies (4, 5).

Animal-free culture systems aim to replace traditional reagents, such as FBS and animal-derived extracellular matrix (ECM) proteins, with alternatives like human serum (HS) and human-derived ECM proteins. While these alternatives offer improved compatibility and reduced immunogenicity compared to their animal counterparts, they are constrained by factors such as availability, variability, and high costs. Consequently, options like defined

serum-free formulations and recombinant ECM proteins, such as iMatrix-511, are being explored to effectively support cell growth and differentiation (1, 6).

Respiratory syncytial virus (RSV) is a leading cause of acute lower respiratory tract infections, particularly in infants, young children, and the elderly, representing a significant global health burden (7). RSV research and the development of antiviral therapies or vaccines often relies on animal models, including mice and cotton rats, to study anti-viral therapies and host-pathogen interactions. However, these do not accurately replicate the virus or reproduce the pathology of disease observed in humans. This lack of translational relevance has contributed to limited major breakthroughs in understanding RSV infection mechanisms or developing effective therapeutic strategies (8, 9).

To address these limitations, more complex *in vitro* models are needed to study viral infection mechanisms and immune involvement. Inverted air-liquid interface (ALI) cultures provide an alternative approach by enabling interactions between epithelial cells and immune cells in a physiologically relevant orientation (10, 11). Despite their advantages, these models present challenges related to cell adhesion and differentiation compared to traditional gravity-assisted conditions, which can affect barrier formation and overall model stability.

In this study, our aim was to demonstrate the feasibility of animal-free cell culture media and substrates for supporting the growth and differentiation of primary paediatric human bronchial epithelial cells (BECs) using the inverted ALI system and for propagating respiratory syncytial virus (RSV) for infection studies. Establishing feasibility in these complex models could pave the way for easier adaptation to simpler traditional models, promoting broader adoption of animal free methods in airway research.

Methods

Animal-free cell attachment and growth

Primary paediatric (2-year-old female Caucasian) bronchial epithelial cells (BECs) were purchased from Epithelix Sàrl (Geneva, Switzerland). While the exact conditions of their initial culture by the supplier are unknown, it is likely that they were not animal-free. BECs were grown on human placenta collagen IV (Merck, Germany) or mammalian-free substrates, specifically jellyfish collagen 0 (Jellagen, Cardiff, UK) or iMatrix-511—a recombinant extracellular matrix protein (AMSBIO, Oxford, UK) or rat tail collagen I (Corning, NY, USA), which is commonly used for cell culture applications. The number of viable cells was determined at 24, 48, 72 and 96 hours by detaching the cells using TrypLE Express (Thermo Fisher Scientific, UK) and counting viable cells using the trypan blue exclusion method, Cell proliferation was also monitored using the zenCELL owl incubator microscope (LabLogic, UK), as shown in **Supplementary Figure 1**. While metabolic

assays like MTT or resazurin could provide additional insights, trypan blue is a validated method for assessing BEC viability (12, 13).

BECs were also grown in two types of media: PromoCell Airway Epithelial Cell Growth Medium (AECGM) (PromoCell, Heidelberg, Germany), which is based on our previous published model (11), or Epithelix hAEC/hSAEC xeno-free culture medium (hAECM/hSAECM, Epithelix Sàrl, Geneva, Switzerland).

Cell propagation and ALI differentiation

Primary paediatric BECs were co-cultured on mitotically inactivated 3T3-J2 feeder cells (14) in primary airway epithelial cell culture medium (3T3-Y conditions) composed of 325ml Dulbecco's Modified Eagle Medium (DMEM), 125ml Ham's F-12 (Thermo Fisher Scientific, Dartford, UK), 9% human serum (HS) (Merck, Darmstadt, Germany), 1% penicillin-streptomycin, 10 µg/ml gentamicin (Thermo Fisher Scientific, UK), 25 ng/ml hydrocortisone (Merck, Germany), 0.125 ng/ml recombinant human epidermal growth factor (EGF) (Thermo Fisher Scientific, UK), 5 µg/ml bovine insulin (I5500, Merck, Darmstadt, Germany), 5 µM Y-27632 Rho-associated coiled-coil kinase (ROCK) inhibitor (Enzo Life Sciences, USA), 250 ng/ml amphotericin B (Thermo Fisher Scientific, UK) and 0.1 nM cholera toxin (Merck, Germany).

BECs were then cultured at air-liquid interface (ALI) in complete PneumaCult™-ALI medium (STEMCELL Technologies, Vancouver, Canada) to promote differentiation, a process that was monitored over a period of 28 days.

Evaluation of barrier integrity

At 28-days post-ALI, the integrity of the epithelial barrier was evaluated using trans-epithelial electrical resistance (TEER) measurements and dextran permeability assays. TEER was measured with an Epithelial Volt/Ohm Meter 3 (EVOM3, World Precision Instruments), adjusting for the membrane area. For dextran permeability, ALI cultures were placed in Hanks' balanced salt solution containing calcium and magnesium (HBSS+/+) plus Texas Red™-dextran (Thermo Fisher Scientific, UK) at 100 µg/ml for 20 minutes in the dark. 100 µl of standards and supernatant were transferred to a solid black 96-well plate in triplicate and fluorescence was measured with a microplate reader at an excitation/emission wavelength of 595/615 nm. A membrane without cells served as a control. The translocated dextran concentration, derived from a standard curve, indicated paracellular permeability.

Ciliary beat frequency

Fast time-lapse videos were acquired using a Nikon Eclipse Ti-E inverted microscope (Nikon, Japan) equipped with an ORCA-Flash4.0 digital CMOS camera (Hamamatsu, Japan) and processed using Fiji image analysis software (15). Ciliary beat frequency (CBF) was then measured with an automated `ciliR` code for fast Fourier transform of the data (using R), as previously described (16).

Flow cytometric analysis

For flow cytometry, ALI cultures were rinsed apically with Dulbecco's phosphate buffered saline (DPBS, Thermo Fisher Scientific, UK) and cells were dissociated from the membrane using TrypLE Express (Thermo Fisher Scientific, UK). Cells were blocked in Human TruStain FcX™ (Biolegend, USA) diluted 1/50 in DPBS for 10 minutes at 4°C to minimise Fc receptor non-specific binding and stained with LIVE/DEAD™ fixable near IR dye to determine the viability of cells (Thermo Fisher Scientific, UK).

Cells were washed by adding 100 µl FACS buffer (1X DPBS, 1% HS, 1 mM EDTA) and centrifuging at 300 x g for 5 minutes, then stained with surface markers CD49f-PE/Dazzle™-594 (BioLegend, San Diego, CA, USA), CD271-BV421 (BD Biosciences, NJ, USA), TSPAN8-BV711 (BD Biosciences, NJ, USA) and CD66c-PE (BD Biosciences, USA) in 50 µl FACS buffer for 20 minutes at 4°C in the dark (**Table 1**). Cells were washed by adding 100 µl FACS buffer and centrifuging at 300 x g for 5 minutes, fixed with 4% (v/v) paraformaldehyde (PFA, Thermo Fisher Scientific, UK) for 20 minutes at 4°C and then permeabilised by washing in permeabilization buffer (Thermo Fisher Scientific, UK). For intracellular staining, cells were resuspended in 50 µl permeabilization buffer containing MUC5AC-FITC (Novus Biologicals, USA) and acetyl-α-Tubulin-Alexa Fluor™ 647 (Cell Signaling Technology, Danvers, Massachusetts, USA) for 20 minutes at 4°C in the dark (**Table 1**). After a final wash in permeabilization buffer, cells were resuspended in 200 µl FACS buffer and analysed using a CytoFLEX S flow cytometer.

Basal cells were defined as the proportion of CD49f/CD271 double positive cells in the live cell population. Ciliated cells were then gated from the non-basal cell population based on acetyl-α-Tubulin^{hi} and CD66c^{lo} expression, whilst goblet cells were further separated from the non-ciliated population based on positive expression for MUC5AC (17).

Fluorescence confocal imaging

ALI cultures were fixed with 4% (v/v) PFA in DPBS for 30 minutes at room temperature, washed twice in DPBS and blocked and permeabilised in 3X Animal-Free Blocker® (Vector Laboratories, Newark, CA, USA) with 0.1% Triton™ X-100 (Merck, Germany) for 1 hour at room temperature. Membranes were then carefully removed using a scalpel and incubated with fluorescently labelled recombinant antibodies diluted in 1X Animal-Free Blocker® with 0.1% Triton™ X-100 for 1 hour at room temperature (**Table 2**). For ciliated cells, membranes were treated with fluorescently labelled wheat germ agglutinin, an animal-free carbohydrate-binding lectin, which has previously been used in studies involving ciliated cells of the respiratory epithelium (18, 19). After 3x washes in DPBS, membranes were incubated with 4′,6-diamidino-2-phenylindole (DAPI) for 10 minutes at room temperature then mounted onto a glass slide with propyl gallate mounting medium (Merck, Germany).

Slides were imaged using a 20X Plan Achromat Objective and a Zeiss LSM710 confocal microscope with the pinhole set at 1 Airy unit (AU).

Viral propagation

Recombinant GFP tagged-RSV A2 strain was kindly provided by Professor Jean-François Eléouët (Unité de Virologie Immunologie Moléculaires, France) (20). RSV propagation was evaluated using Human Epithelial Type 2 (HEp-2, CCL-23™) cells from ATCC (Virginia, US). These were maintained in VP-SFM (Thermo Fisher Scientific, UK) supplemented with 4 mM L-glutamine (Thermo Fisher Scientific, UK) and 0.5% penicillin-streptomycin for virus production or DMEM with 2% HS and 0.5% penicillin-streptomycin for viral quantification. The efficiency of RSV infection and replication was assessed by quantifying viral titres at different time points post-infection. This approach was designed to test the efficacy of serum-free medium in supporting viral growth and to compare it with traditional serum-containing medium.

BD cytometric bead array analysis

This assay was carried out using a cytometric bead array (CBA) (BD Biosciences, USA); antibody-coated beads of known size and fluorescence are used to detect multiple proteins in each sample. This assay was carried out as described in the manufacturer's protocol, to quantify human cytokines such as Human IL-6 (A7, 558276, BD Biosciences), Human IL-8 (A9, 558277, BD Biosciences) and Human IP-10 (B5, 558280, BD Biosciences), in supernatant obtained from mock- or RSV-infected cultures. Test samples were diluted 1/10 in assay diluent to ensure their median fluorescence values fall within the range of the generated standard curve. 50 µl of each standard and test

sample were incubated with 50 µl mixed capture beads for 1 hour at room temperature on an orbital shaker. 50 µl mixed PE detection reagent was then added to each assay tube for a further 2 hours. Beads were washed by adding 50 µl wash buffer (1X DPBS, 1% HS, 0.09% sodium azide) and centrifuging at 200 x g for 5 minutes. Beads were resuspended in 200 µl wash buffer and analysed using a BD FACSymphony A5 flow cytometer.

Real-Time quantitative PCR for RSV detection

Viral RNA was extracted from supernatant using the QIAamp Viral RNA Mini Kit (Qiagen, Germany) as per the manufacturer's instructions and quantified with a Thermo Scientific Nanodrop 1000 (Thermo Fisher Scientific, UK). 100 ng total RNA was then used to synthesise cDNA using the High-Capacity RNA-to-cDNA Kit (Thermo Fisher Scientific, UK) in a final reaction volume of 40 µl. Real-Time Quantitative PCR (RT-qPCR) was performed using TaqMan Universal Master Mix II, with UNG (Thermo Fisher Scientific, UK) containing specific primers for RSV-A N protein and a fluorescently labelled probe (**Table 3**) (21). Primers and probe were used at final concentrations of 900 nM and 250 nM, respectively. Samples were run on an AB Biosystems StepOnePlus Real-Time PCR System (Thermo Fisher Scientific, UK); cDNA was denatured at 95°C for 10 minutes and amplified by 40 cycles (95°C for 15 seconds and 60°C for 1 minute). Viral load was extrapolated from a standard curve generated by performing ten-fold serial dilutions of a plasmid containing the N protein sequence starting at $1x10^6$ copies to 1 copy (22).

Data analysis

Data from cell viability assays, TEER measurements, and viral titres were statistically analysed using ANOVA and mixed-effects models to compare the performance of animal-free systems with traditional methods. The primary focus was on cell viability, differentiation efficiency, TEER values, and RSV propagation efficiency. Flow cytometry data were analysed using FlowJo v10 (Tree Star Inc., San Carlos, CA, USA).

Results

Jellyfish collagen 0 best supports human BEC attachment.

To determine alternative ECM substrates for the expansion of human airway epithelial cells, primary paediatric BECs were first cultured on different ECM proteins in PromoCell AECGM. These included the standard rat tail collagen I, commonly used for ALI culture, human placenta collagen IV and two alternatives of non-mammalian ECM: jellyfish collagen 0 and iMatrix-511, which is recombinantly expressed in an epithelial cell line.

The adhesion of BECs at 24-, 48-, 72- and 96-hours post-seeding was assessed by detaching adherent cells and counting viable cells using the trypan blue exclusion method (**Figure 1a**). We recovered more viable BECs from plates coated in jellyfish collagen 0 at 48, 72 and 96 hours (mean ± SEM of 118,000 ± 13,653, 119,333 ± 10,503 and 112,501 ± 13,276 cells/ml) in comparison to plates coated in rat tail collagen I (73,333 ± 13,844 and 70,833 ± 9,075 cells/ml), human placenta collagen IV (65,333 ± 7566 cells/ml) and iMatrix-511 (66,000 ± 10,570 and 66,000 ± 5033 cells/ml) ($p<0.05$, N = 6 independent experiments). We found no difference in the number of recovered BECs grown on rat tail collagen I compared to either human placenta collagen IV or iMatrix-511.

BECs were also assessed using brightfield microscopy, with no noticeable changes in cell morphology detected between the cell attachment substrates (**Figure 1b**).

In summary, human BECs can attach to plates coated in extracellular matrix-derived from human and non-mammalian sources with no negative impact on cell viability or morphology. Since BECs adhered in greater numbers to jellyfish collagen 0 compared to the standard rat tail collagen I and other cell attachment substrates tested, this substrate was used for subsequent comparison studies.

Animal-free medium supports BEC culture but less effectively than a 3T3+Y feeder cell-based method.

The growth of primary paediatric BECs in different animal-free culture media, including PromoCell AECGM, Epithelix hAECM, hSAECM, and the 3T3+Y method supplemented with human serum (HS) was then investigated. Cell viability was quantified at 24, 48, 72 and 96 hours using the trypan blue exclusion method. The findings indicate significantly higher numbers of viable BECs across all timepoints when cultured using the 3T3+Y method supplemented with human serum (HS) (152,889 ± 10,536, 244,444 ± 20,314, 272,889 ± 26,548 and 348,444 ± 37,217 cells/ml) compared to the other growth media tested ($p<0.05$, N = 9 independent experiments; **Figure 2a**) (14, 23). Additionally, the

number of viable BECs in Epithelix hAECM were also significantly greater at 72 and 96 hours (170,222 ± 19,103 and 159,111 ± 18,255 cells/ml) compared to hSAECM (88,444 ± 10,943 and 100,444 ± 7,985 cells/ml) ($p<0.05$, N = 9 independent experiments). No significant differences were observed in growth between BECs maintained in PromoCell AECGM and those in either Epithelix hAECM or hSAECM. This was confirmed by capturing real-time phase-contrast images and using automated image processing algorithms (**Supplementary Figure 1**).

Cell morphology was also assessed using brightfield microscopy; BECs grown on a feeder layer in 3T3+Y conditions exhibited a characteristic cobblestone-like appearance with small epithelial colonies, while BECs cultured on jellyfish collagen 0 in either PromoCell AECGM, Epithelix hAECM or hSAECM were larger and did not form compact cell clusters (**Figure 2b**).

In summary, we found that human BECs can be cultured to comparable cell numbers using different animal-free media, but the number of viable cells was approximately half that achieved with the 3T3+Y method. Given the importance of attaining optimal phenotypic and functional endpoints, such as differentiation, CBF, and TEER, BECs cultured under 3T3+Y conditions supplemented with human serum are recommended for further cell propagation.

Animal-free matrix proteins support epithelial cell differentiation at ALI, with optimal ciliation observed on human placenta collagen IV.

To evaluate whether the use of animal-free components affects the capacity of human BECs to differentiate into ciliated epithelial cells - the target of RSV infection (24) - BECs grown in 3T3+Y conditions or cultured on jellyfish collagen 0 in Epithelix hAECM were seeded on membrane inserts coated with either rat tail collagen I, human placenta collagen IV and jellyfish collagen 0. We found that BECs that had been cultured on jellyfish collagen 0 in Epithelix hAECM did not adhere to the collagen-coated membrane inserts with the cells detaching upon removal of the apical medium during the air-lifting process (data not shown). BECs grown in 3T3+Y conditions survived up to 4 weeks at ALI, but exhibited either no ciliation on jellyfish collagen 0, low level ciliation (<5 areas with motile cilia) on rat tail collagen I or high level ciliation (>5 areas with motile cilia) on human placenta collagen IV as based on previously established morphological criteria and observed under phase contrast microscopy (25) (**Table 3**). A representative slow-motion video of cells grown on human placenta collagen IV is shown in Video 1.

However, human BECs differentiated on human placenta collagen IV-coated membrane inserts remained adhered and, after 4 weeks, exhibited a mean TEER value of 180.7 ± 6.7 $\Omega \cdot cm^2$ (**Figure 3a**). Although this was significantly lower than the 348.2 ± 61.8 $\Omega \cdot cm^2$ reported in our previous animal-component-based model, which included an additional Matrigel (mouse-derived) layer (11), it was significantly higher than the blank, which indicates that the animal-free model still establishes a restrictive epithelial barrier. This was further supported by a reduced permeability to 3 kDa Texas Red-dextran (5.3 ± 0.8 µg/ml) compared to empty membrane inserts (12.6 ± 0.5 µg/ml) ($p<0.0001$, N = 8 independent experiments; **Figure 3b**). Beating cilia were observed (Video 1), indicating cell differentiation and polarisation and CBF was quantified via high-speed video microscopy, revealing that approximately 20% of ROIs had active cilia, and a mean CBF of 7.66 ± 1.95 Hz (**Figure 3c-e**).

Flow cytometry analysis quantified the proportions of basal, ciliated and goblet cells in the ALI cultures, as described previously (17). The cell gating technique is show in **Figure 3f.** The proportions of each cell type were calculated from the total number of cells acquired per well, with basal cells (CD49f+ CD271+) making up approximately 18% (4,001 ± 115 cells), ciliated cells (acetyl-α-Tubulin^{hi} CD66c^{lo}) around 7% (1,557 ± 488 cells) and goblet cells (MUC5AC+) about 2% (549 ± 519 cells) of the total cell population (21,951 ± 1,400 cells) (**Figure 3g**). Other distinct populations were identified, including acetyl-α-Tubulin+ CD66c+ non-basal cells and MUC5AC- non-ciliated cells, which are likely to represent secretory and intermediate progenitor populations for ciliated and goblet cells as revealed by single-cell RNA sequencing of human AECs during *in vitro* ALI differentiation (26). The functional identity and homogeneity of these populations remain unclear and thus they were excluded from further analysis. ALI cultures were also stained for expression of cell type markers using animal-free reagents. However, the resulting staining was weaker than expected and requires further optimisation (preliminary staining shown in Supplementary Figure 2).

In summary, human BECs were able to differentiate into multiple specialised cell types, including ciliated and goblet cells, when grown at ALI on human placenta collagen-IV coated membranes (i.e. in animal-free conditions). This model enables the epithelial layer of the human airway to be the unit of study, allowing for the investigation of disease mechanisms during RSV infection, which preferentially target ciliated epithelial cells (27).

VP-SFM supports RSV production in HEp-2 cells and successful infection of differentiated BECs in ALI cultures.

The next stage was to assess whether alternative animal-free medium could support viral replication by the host cells and subsequent production of viral stocks for cell-infectivity

assays and anti-viral testing. Results showed that HEp-2 cells had a significantly higher viability in DMEM supplemented with 2% FBS at later timepoints (48 hours: 296,670 ± 16,670 cells/ml; 72 hours: 353,330 ± 50,440 cells/ml; and 96 hours: 640,000 ± 46,190 cells/ml) compared to VP-SFM (48 hours: 80,000 ± 5,770 cells/ml, 72 hours: 183,330 ± 40,960 cells/ml, and 96 hours: 263,330 ± 49,780 cells/ml) ($p<0.05$, N = 3 technical repeats; **Figure 4a**). Additionally, HEp-2 cells cultured in VP-SFM underwent morphological changes, appearing more elongated and fibroblast-like compared to parental HEp-2 cells maintained in 2% FBS (**Figure 4b**).

These cells were also tested for their susceptibility to infection with recombinant GFP-tagged RSV. Surprisingly, we found that despite their reduced growth in VP-SFM, HEp-2 cells showed a significantly higher number of infected, GFP-positive cells at 72 and 120 hours (63 ± 9 and 133 ± 20 cells) compared to those maintained in 2% FBS (18 ± 1 and 45 ± 8 cells) ($p<0.05$, N = 6 technical repeats; **Figure 4c**).

Furthermore, we found that RSV propagated in HEp-2 cells cultured in VP-SFM could infect differentiated BECs grown at ALI that were also grown under animal-free conditions. At 24 hours post-infection GFP-positive cells were readily detected in RSV-infected BECs, while no GFP signal was observed in the mock-infected control (**Figure 4d**). Apical supernatant from mock- and RSV-infected BECs were collected and analysed by RT-qPCR and flow cytometry to quantify viral RNA. As expected, a significantly higher viral load was detected in the apical supernatant of RSV-infected BECs ($1.5x10^6 \pm 6.8x10^5$ copies/µl), indicating the presence of virus, compared to mock-infected control cells (20.7 ± 3.6 copies/µl) (**Figure 4e**). RSV infection also led to a significantly higher concentration of IL-6 and IL-8 in the apical supernatant of RSV-infected BECs (3,124 ± 860 and 3,119 ± 1,091 pg/ml) compared to mock-infected control cells (2.5 ± 2.3 and 118 ± 62.7 pg/ml, respectively) (**Figure 4f**). No differences were observed in the levels of IP-10 in the apical supernatant of mock- or- RSV-infected BECs. Together, these findings support the use of VP-SFM as a viable animal-free alternative for culturing HEp-2 cells and producing RSV for research purposes.

Discussion

The aim of this study was to replace the use of animal-derived media and substrates in the culture of a human relevant *in vitro* model to study RSV infection. Different commercially available cell attachment substrates and culture media were investigated for growing human BECs and HEp2 cells.

Our findings highlight the potential use of jellyfish collagen 0 and human recombinant laminin-511 as alternatives to the traditionally used rat tail collagen I in the culture of primary BECs. These alternatives not only support comparable cell attachment but also address the ethical and safety concerns associated with mammalian collagen. Jellyfish collagen 0 has previously been used to successfully culture multiple cell types including human primary cells and stem cells with comparable immunogenic responses and cytokine release profiles to mammalian collagen *in vitro* (28). Human recombinant laminin-511, on the other hand, enables feeder-free culture and provides superior adhesion of human-induced pluripotent stem cells (hiPSCs) and human embryonic stem cells (hESCs) than full-length laminin or Matrigel™ (29).

While jellyfish collagen 0 showed promise as an alternative for growing human BECs in 2D culture, it was unsuitable for differentiating BECs at the air-liquid interface (ALI), as cells detached from the membrane upon removal of the apical medium. This may be due to morphological differences between human BECs grown in monoculture, which are larger and less compact, compared to those co-cultured with feeder cells and treated with Y-27632 (a ROCK inhibitor), which are compacted by the fibroblast colonies as shown in **Figure 2b**. These findings suggests that the culture conditions, including the quality of expanded basal BECs, influence cell survival and differentiation potential. Indeed, Y-27632 has been shown to enhance basal BEC proliferation *in vitro* without compromising subsequent ciliated epithelial differentiation (30, 31). This effect is associated with cell rounding, reduced cell size, and the localization of E-cadherin and actin at cell-cell junctions upon confluence (30). As the composition of most commercially available culture media is proprietary, it is difficult to conclude whether the differences observed here are due to any one factor or component in the media. However, in our study, human BECs treated with Y-27632 in the presence of a 3T3-J2 feeder layer provided the most optimal conditions for achieving phenotypic and functional endpoints. While the 3T3-J2 feeder cells were cultured in medium supplemented with human serum, their initial derivation involved bovine serum (14). The extent to which human serum affects long-term feeder cell function warrants further investigation.

Paediatric BECs that were differentiated at ALI in the animal-free culture conditions exhibited lower TEER at 4 weeks post-ALI (~200 $\Omega*cm^2$) compared to those previously reported using adult nasal AECs (>300 $\Omega*cm^2$) and human airway tissue (trachea and mainstem bronchi, ~500 $\Omega*cm^2$) (11, 32, 33). Despite this, they achieved some barrier function, reducing paracellular permeability of fluorescently labelled dextran, and

showed evidence of specialised cell types, such as ciliated and goblet cells. CBF measurements at 4 weeks post-ALI (7.66 ± 1.95 Hz) were reduced compared to the reported range for nasal cilia (12-16 Hz), but were within range compared to CBF from nasal brush biopsies (4.25-11.63 Hz), human BECs differentiated in PneumaCult™-ALI medium (10.44 ± 0.93 Hz) and brushings from the proximal bronchi of resected lungs (7.1 ± 1.29 Hz) (34-37). It is worth mentioning that CBF can be affected by environmental factors, for instance, increasing temperatures have been associated with increased CBF in nasal brushings, while CBF slows down in aging ciliated nasal AECs (38-40). The exact numbers of ciliated and goblet cells in the differentiated epithelium are highly donor dependent. Further experiments using a larger sample size of paediatric BEC donors would provide a more comprehensive understanding of how donor-to-donor variability impacts cellular composition and differentiation capacity in this animal-free model.

Our results demonstrate that RSV propagated in animal-free VP-SFM efficiently infects differentiated BECs and induced a robust inflammatory response, with elevated IL-6 and IL-8 levels in the apical supernatant. Although no direct side-by-side experiments with FCS-containing media were performed, these results are consistent with previous studies showing that RSV infection induces a strong epithelial pro-inflammatory cytokine response (32, 41-44).

Conclusion

Animal-free cell culture systems, including serum-free media and human ECM proteins, offer a promising alternative to traditional animal-derived components. While challenges in differentiation and barrier integrity exist, the ability of these systems to support cell growth and enhance viral propagation highlights their potential for research and therapeutic applications. Importantly, our findings demonstrate that replacing animal-derived components in cell culture systems with animal-free reagents supports effective viral propagation and differentiation of primary airway epithelial cells, highlighting their potential for animal-free reagents in studying RSV pathogenesis and antiviral testing. Further optimization and validation of these methods will contribute to more ethical, reproducible, and human-relevant *in vitro* models.

Acknowledgements

The authors thank Dr Ayad Eddaoudi (UCL GOS ICH Flow Cytometry Core Facility) for assistance with flow cytometry. This study was funded by Animal Free Research UK (AFR19-20274) and was carried out in accordance with the terms and conditions as stated in document number GH2019-TC/v1.1/27.01.2020. This work was also supported by grants from UKRI/ BBSRC (BB/V006738/1) and the NIHR Great Ormond Street Hospital Biomedical Research Centre. The views expressed are those of the author(s) and not necessarily those of the NHS, the NIHR or the Department of Health.

Author contributions

All authors declare no conflicts of interest.

M.P., designed the study, conducted experiments, analysed data, and prepared the manuscript. E.K.H. and C.O.C assisted with flow cytometric analysis. J.H contributed to data acquired from non-AF ALI model. R.L.S. and P.D.C., provided support through interpretation of data and review of manuscript. R.E.H. contributed to study design, supervised data analysis, interpretation, and manuscript preparation. C.M.S conceived the study, oversaw funding, contributed to study design, supervised data analysis, interpretation, and manuscript preparation.

References

1. Weber T, Wiest J, Oredsson S, Bieback K. Case Studies Exemplifying the Transition to Animal Component-free Cell Culture. Altern Lab Anim. 2022;50(5):330-8.
2. Wadman M. FDA no longer has to require animal testing for new drugs. Science. 2023;379(6628):127-8.
3. Loewa A, Feng JJ, Hedtrich S. Human disease models in drug development. Nat Rev Bioeng. 2023:1-15.
4. Grimm H, Biller-Andorno N, Buch T, Dahlhoff M, Davies G, Cederroth CR, et al. Advancing the 3Rs: innovation, implementation, ethics and society. Front Vet Sci. 2023;10:1185706.
5. Hoang DM, Pham PT, Bach TQ, Ngo ATL, Nguyen QT, Phan TTK, et al. Stem cell-based therapy for human diseases. Signal Transduct Target Ther. 2022;7(1):272.
6. Canovas D, Bird N. Human AB serum as an alternative to fetal bovine serum for endothelial and cancer cell culture. ALTEX. 2012;29(4):426-8.
7. Shi T, McAllister DA, O'Brien KL, Simoes EAF, Madhi SA, Gessner BD, et al. Global, regional, and national disease burden estimates of acute lower respiratory infections due to respiratory syncytial virus in young children in 2015: a systematic review and modelling study. Lancet. 2017;390(10098):946-58.
8. Renn M, Bartok E, Zillinger T, Hartmann G, Behrendt R. Animal models of SARS-CoV-2 and COVID-19 for the development of prophylactic and therapeutic interventions. Pharmacol Ther. 2021;228:107931.
9. Taylor G. Animal models of respiratory syncytial virus infection. Vaccine. 2017;35(3):469-80.
10. Deng Y, Herbert JA, Smith CM, Smyth RL. An in vitro transepithelial migration assay to evaluate the role of neutrophils in Respiratory Syncytial Virus (RSV) induced epithelial damage. Sci Rep. 2018;8(1):6777.
11. Herbert JA, Deng Y, Hardelid P, Robinson E, Ren L, Moulding D, et al. beta2-integrin LFA1 mediates airway damage following neutrophil transepithelial migration during respiratory syncytial virus infection. Eur Respir J. 2020;56(2).
12. Kelsen SG, Mardini IA, Zhou S, Benovic JL, Higgins NC. A technique to harvest viable tracheobronchial epithelial cells from living human donors. Am J Respir Cell Mol Biol. 1992;7(1):66-72.
13. Maestre-Batlle D, Pena OM, Hirota JA, Gunawan E, Rider CF, Sutherland D, et al. Novel flow cytometry approach to identify bronchial epithelial cells from healthy human airways. Sci Rep. 2017;7:42214.
14. Butler CR, Hynds RE, Gowers KH, Lee Ddo H, Brown JM, Crowley C, et al. Rapid Expansion of Human Epithelial Stem Cells Suitable for Airway Tissue Engineering. Am J Respir Crit Care Med. 2016;194(2):156-68.
15. Schindelin J, Arganda-Carreras I, Frise E, Kaynig V, Longair M, Pietzsch T, et al. Fiji: an open-source platform for biological-image analysis. Nat Methods. 2012;9(7):676-82.
16. Grant O, Larken I, Reitemeier S, Mitchison HM, Dawes W, Phillips A, et al. ciliR: a new R package for determining ciliary beat frequency using fast-Fourier transformation. bioRxiv. 2023:2023.12.20.572306.

17. Bonser LR, Koh KD, Johansson K, Choksi SP, Cheng D, Liu L, et al. Flow-Cytometric Analysis and Purification of Airway Epithelial-Cell Subsets. Am J Respir Cell Mol Biol. 2021;64(3):308-17.
18. Menco BP. Lectins bind differentially to cilia and microvilli of major and minor cell populations in olfactory and nasal respiratory epithelia. Microsc Res Tech. 1992;23(2):181-99.
19. Nakamura R, Katsuno T, Kishimoto Y, Kaba S, Yoshimatsu M, Kitamura M, et al. A novel method for live imaging of human airway cilia using wheat germ agglutinin. Sci Rep. 2020;10(1):14417.
20. Fix J, Galloux M, Blondot ML, Eleouet JF. The insertion of fluorescent proteins in a variable region of respiratory syncytial virus L polymerase results in fluorescent and functional enzymes but with reduced activities. Open Virol J. 2011;5:103-8.
21. Dewhurst-Maridor G, Simonet V, Bornand JE, Nicod LP, Pache JC. Development of a quantitative TaqMan RT-PCR for respiratory syncytial virus. J Virol Methods. 2004;120(1):41-9.
22. Castagne N, Barbier A, Bernard J, Rezaei H, Huet JC, Henry C, et al. Biochemical characterization of the respiratory syncytial virus P-P and P-N protein complexes and localization of the P protein oligomerization domain. J Gen Virol. 2004;85(Pt 6):1643-53.
23. Hynds RE, Butler CR, Janes SM, Giangreco A. Expansion of Human Airway Basal Stem Cells and Their Differentiation as 3D Tracheospheres. Methods Mol Biol. 2019;1576:43-53.
24. Kuek LE, Lee RJ. First contact: the role of respiratory cilia in host-pathogen interactions in the airways. Am J Physiol Lung Cell Mol Physiol. 2020;319(4):L603-L19.
25. Smith CM, Kulkarni H, Radhakrishnan P, Rutman A, Bankart MJ, Williams G, et al. Ciliary dyskinesia is an early feature of respiratory syncytial virus infection. Eur Respir J. 2014;43(2):485-96.
26. Ruiz Garcia S, Deprez M, Lebrigand K, Cavard A, Paquet A, Arguel MJ, et al. Novel dynamics of human mucociliary differentiation revealed by single-cell RNA sequencing of nasal epithelial cultures. Development. 2019;146(20).
27. Villenave R, Thavagnanam S, Sarlang S, Parker J, Douglas I, Skibinski G, et al. In vitro modeling of respiratory syncytial virus infection of pediatric bronchial epithelium, the primary target of infection in vivo. Proc Natl Acad Sci U S A. 2012;109(13):5040-5.
28. Ahmed Z, Powell LC, Matin N, Mearns-Spragg A, Thornton CA, Khan IM, et al. Jellyfish Collagen: A Biocompatible Collagen Source for 3D Scaffold Fabrication and Enhanced Chondrogenicity. Mar Drugs. 2021;19(8).
29. Miyazaki T, Futaki S, Suemori H, Taniguchi Y, Yamada M, Kawasaki M, et al. Laminin E8 fragments support efficient adhesion and expansion of dissociated human pluripotent stem cells. Nat Commun. 2012;3:1236.
30. Horani A, Nath A, Wasserman MG, Huang T, Brody SL. Rho-associated protein kinase inhibition enhances airway epithelial Basal-cell proliferation and lentivirus transduction. Am J Respir Cell Mol Biol. 2013;49(3):341-7.
31. Witkowski TA, Li B, Andersen JG, Kumar B, Mroz EA, Rocco JW. Y-27632 acts beyond ROCK inhibition to maintain epidermal stem-like cells in culture. J Cell Sci. 2023;136(17).
32. Robinson E, Herbert JA, Palor M, Ren L, Larken I, Patel A, et al. Trans-epithelial migration is essential for neutrophil activation during RSV infection. J Leukoc Biol. 2023;113(4):354-64.

33. Yonker LM, Mou H, Chu KK, Pazos MA, Leung H, Cui D, et al. Development of a Primary Human Co-Culture Model of Inflamed Airway Mucosa. Sci Rep. 2017;7(1):8182.
34. Clary-Meinesz C, Mouroux J, Huitorel P, Cosson J, Schoevaert D, Blaive B. Ciliary beat frequency in human bronchi and bronchioles. Chest. 1997;111(3):692-7.
35. Leung C, Wadsworth SJ, Yang SJ, Dorscheid DR. Structural and functional variations in human bronchial epithelial cells cultured in air-liquid interface using different growth media. Am J Physiol Lung Cell Mol Physiol. 2020;318(5):L1063-L73.
36. Raidt J, Wallmeier J, Hjeij R, Onnebrink JG, Pennekamp P, Loges NT, et al. Ciliary beat pattern and frequency in genetic variants of primary ciliary dyskinesia. Eur Respir J. 2014;44(6):1579-88.
37. Yaghi A, Dolovich MB. Airway Epithelial Cell Cilia and Obstructive Lung Disease. Cells. 2016;5(4).
38. Smith CM, Hirst RA, Bankart MJ, Jones DW, Easton AJ, Andrew PW, et al. Cooling of cilia allows functional analysis of the beat pattern for diagnostic testing. Chest. 2011;140(1):186-90.
39. Ho JC, Chan KN, Hu WH, Lam WK, Zheng L, Tipoe GL, et al. The effect of aging on nasal mucociliary clearance, beat frequency, and ultrastructure of respiratory cilia. Am J Respir Crit Care Med. 2001;163(4):983-8.
40. Nikolaizik W, Hahn J, Bauck M, Weber S. Comparison of ciliary beat frequencies at different temperatures in young adults. ERJ Open Res. 2020;6(4).
41. Diaz PV, Gaggero AA, Pinto RA, Mamani R, Uasapud PA, Bono MR. [Levels of inflammatory cytokines and plasma cortisol in respiratory syncytial virus bronchiolitis]. Rev Med Chil. 2013;141(5):574-81.
42. Tabarani CM, Bonville CA, Suryadevara M, Branigan P, Wang D, Huang D, et al. Novel inflammatory markers, clinical risk factors and virus type associated with severe respiratory syncytial virus infection. Pediatr Infect Dis J. 2013;32(12):e437-42.
43. Villenave R, O'Donoghue D, Thavagnanam S, Touzelet O, Skibinski G, Heaney LG, et al. Differential cytopathogenesis of respiratory syncytial virus prototypic and clinical isolates in primary pediatric bronchial epithelial cells. Virol J. 2011;8:43.
44. McNamara PS, Flanagan BF, Hart CA, Smyth RL. Production of chemokines in the lungs of infants with severe respiratory syncytial virus bronchiolitis. J Infect Dis. 2005;191(8):1225-32.

Table 1. Antibodies used for flow cytometric analysis of differentiated BECs.

Antibody	Target	Fluorophore	Supplier	Host	Animal-derived	Dilution
CD49f (ITGA6)	Basal	PE-Dazzle™ -594	BioLegend (313626)	Rat	Yes*	1/50
CD271 (NGFR)	Basal	BV421	BD Biosciences (562562)	Mouse	Yes*	1/20
TSPAN8	Goblet	BV711	BD Biosciences (748227)	Rat	Yes*	1/100
CD66c	Secretory	PE	BD Biosciences (551478)	Mouse	Yes*	1/100
MUC5AC	Goblet	FITC	Novus Biologicals (NBP2-32732AF488)	Mouse	Yes*	1/50
Acetyl-α-Tubulin	Ciliated	Alexa Fluor™ 647	Cell Signaling Technology (81502)	Rabbit	Yes*	1/50

*To allow direct comparisons to previously published work.

Table 2. Antibodies or conjugate used for IF staining.

Antibody/Conjugate	Target	Fluorophore	Supplier	Animal-derived	Dilution
Keratin 5 (KRT5)	Basal Cells	APC	Miltenyi Biotec (130-127-016)	No	1/50
MUC5AC	Goblet Cells	PE	Miltenyi Biotec (130-127-552)	No	1/50
Wheat Germ Agglutinin (WGA)	Ciliated Cells	Fluorescein	2BScientific (FL-1021-5)	No	1/100

Table 3. Primers and probes used for RSV RT-qPCR.

Primer/Probe	Sequence 5'-3'
RSV-A Forward Primer	CTCAATTTCCTCACTTCTCCAGTGT
RSV-A Reverse Primer	CTTGATTCCTCGGTGTACCTCTGT
RSV-A Probe	[6FAM] TCCCATTATGCCTAGGCCAGCAGCA [TAMRA]

Table 4. Differentiation of inverted ALI cultures.

Cell Attachment Substrate	Level of Ciliation
Rat Tail Collagen I	+
Human Placenta Collagen IV	++
Jellyfish Collagen 0	-

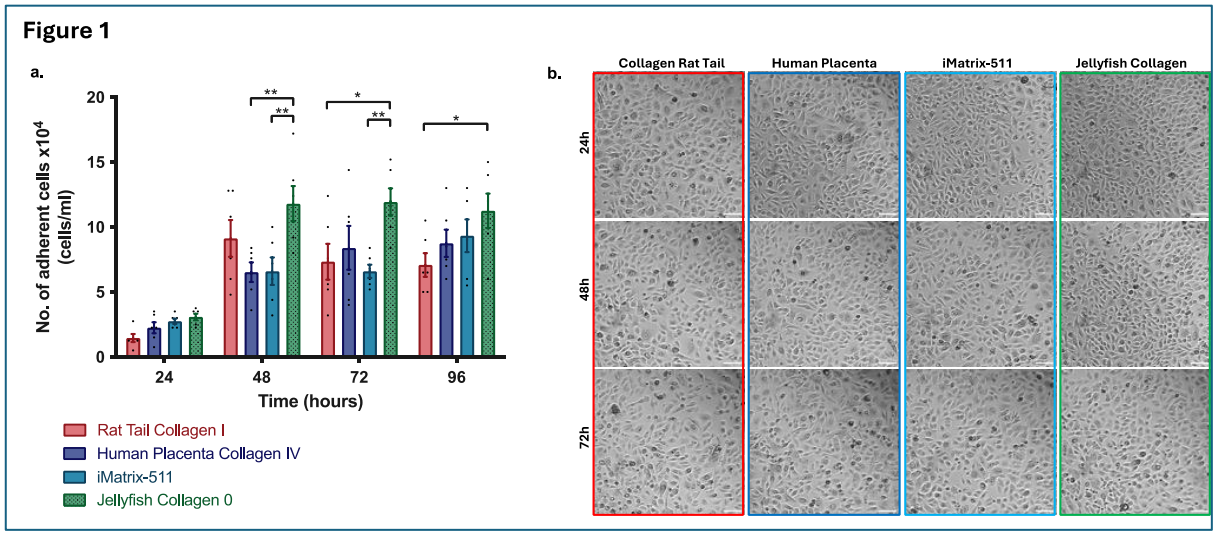

*Figure 1 Comparing animal-free and conventional (rat-tail collagen) substrates for bronchial epithelial cell (BEC) attachment. BECs were grown on different surfaces: rat tail collagen I, human placenta collagen IV, jellyfish collagen 0 and iMatrix-511. a. Number of adherent BECs at 24, 48, 72 and 96 hours. Error bars represent mean ± SEM of N = 6 independent experiments. *p < 0.05, **p < 0.01 (Two-way ANOVA with Tukey post-hoc test). b. Representative timelapse phase-contrast images at 24-72 hours post seeding. Scale bars = 100 µm.*

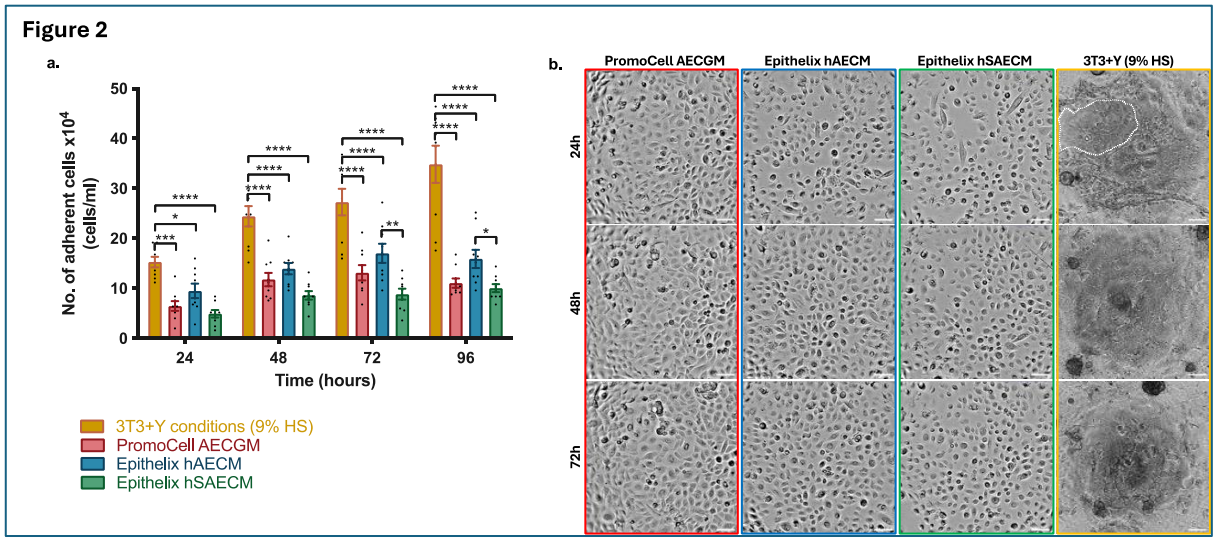

Figure 2 *Primary paediatric BECs can be cultured in human serum or animal-free media. BECs were either grown in co-culture with feeder cells in 3T3+Y +9%HS conditions (gold bars) or on jellyfish collagen 0 using two types of media: PromoCell AECGM (red bars) or Epithelix hAECM/hSAECM (blue/green bars). a. Number of adherent BECs at 24, 48, 72 and 96 hours. Error bars represent mean ± SEM of N = 9 independent experiments. *p < 0.05, **p < 0.01, ***p<0.001, ****p < 0.0001 (Two-Way ANOVA with Tukey post-hoc test). b. Representative timelapse phase-contrast images at 24-72 hours. BECs exhibited a cobblestone-like morphology (dotted line) in co-culture with 3T3-J2 feeder cells. Scale bars =* ***100 µm.***

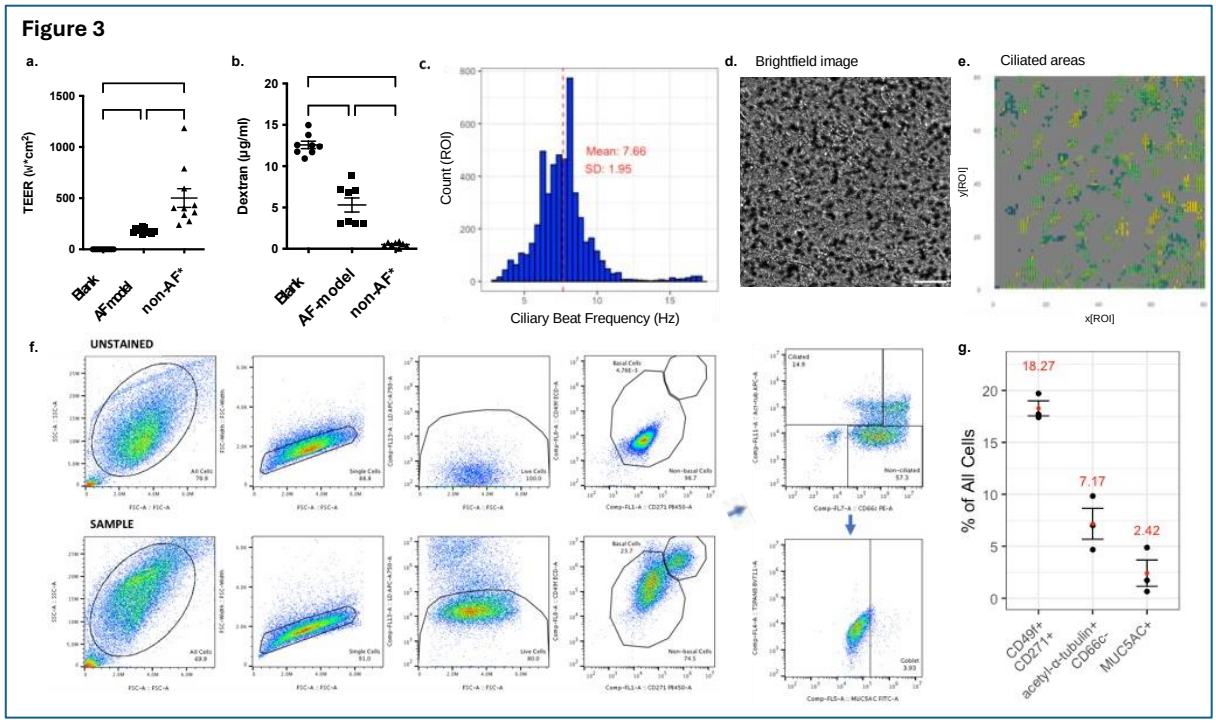

*Figure 3 Barrier integrity and ciliated epithelial cell differentiation of human BECs at ALI. a/b. Epithelial integrity of BECs differentiated from one donor at ALI on membrane inserts coated with human placenta collagen IV for 4 weeks (n=8) compared to our non-AF model (n= 10)(11) that contains an additional Matrigel (mouse derived) layer. Barrier integrity was measured by TEER (Ω*cm²) (a) and dextran permeability (µg/ml) (b). Error bars represent mean ± SEM of N = 8-10 independent Transwells. *p < 0.05 (Unpaired Anova with Benjamini-Hochberg correction for multiple comparisons). c. Histogram of CBF (Hz) was quantified via high-speed video microscopy of 6400 ROI from 5 independent areas (one AEC donor). The red dotted line represents the mean CBF value of all areas. d/e. Representative brightfield image (d) and activity map (e) of one area (field of view) to show the position and distribution of motile ciliated cells. Scale bar = 50 µm. f Example flow cytometry gating strategy to determine the population of basal, ciliated and goblet cells in inverted ALI cultures. Basal cells were defined as the proportion of CD49f/CD127 double positive cells in the live cell population. Ciliated cells were then gated from the non-basal cell population based on acetyl-α-Tubulin⁺ and CD66c⁻ expression, whilst goblet cells were further separated from the non-ciliated population based on positive expression for MUC5AC. g. Proportion (%) of basal (CD49f+ CD271+), ciliated (acetyl-α-Tubulin⁺ CD66c⁻) and goblet (MUC5AC⁺) cells from one AEC donor (n=3 wells). Red dot and error bars represent mean ± SEM of N = 3 wells.*

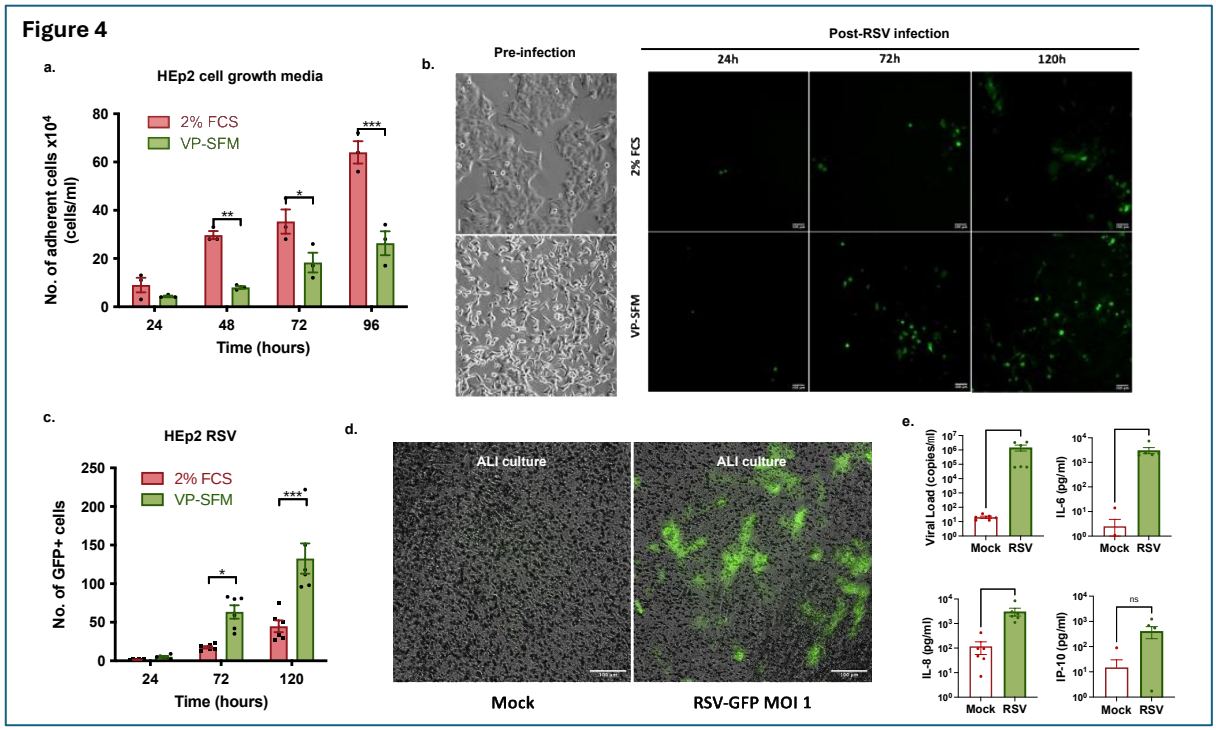

*Figure 4 RSV propagation and ALI culture infection in animal-free conditions. a. Number of adherent Hep-2 cells at 24, 48, 72 and 96 hours. Hep-2 cells were cultured in either DMEM supplemented with 2% FBS or VP-SFM. b. Representative phase-contrast images of Hep2 pre-infection at 48 hours post seeding and representative fluorescent microscopy images to show GFP expression at 24-, 72- and 120-hours post-infection (MOI 0.01). c. The number of GFP-positive cells counted using ImageJ. Error bars represent mean ± SEM of N = 3 donors and 6 technical repeats. *p < 0.05, **p<0.01, ***p < 0.001 (Two-Way ANOVA with Bonferroni correction). Scale bars = 100 µm. d. Representative fluorescent microscopy images of mock- and RSV-infected BEC grown at ALI at 24 hours post-infection (MOI 1). Scale bars = 100 µm. e. RT-qPCR analysis to determine RSV copy number in the apical supernatant of mock- and RSV-infected BECs at 24 hours. Boxplots show viral load (copies/µl). The red dashed line represents the threshold for detecting the virus. f. Cytokine analysis of IL-6, IL-8 and IP-10 in the apical supernatant of mock- and RSV-infected BECs at 24 hours. and concentration (pg/ml) of N = 6 independent experiments. *p < 0.05 (Wilcoxon signed-rank test).*

Supplementary Figure 1

a.

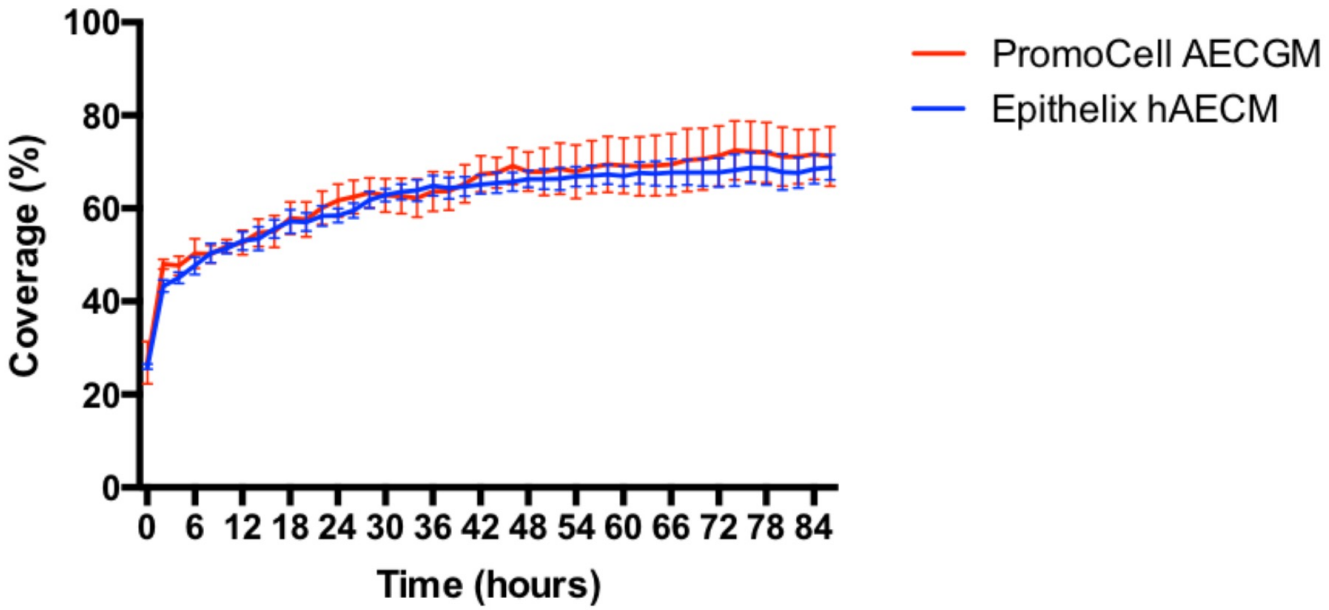

b.

PromoCell AECGM

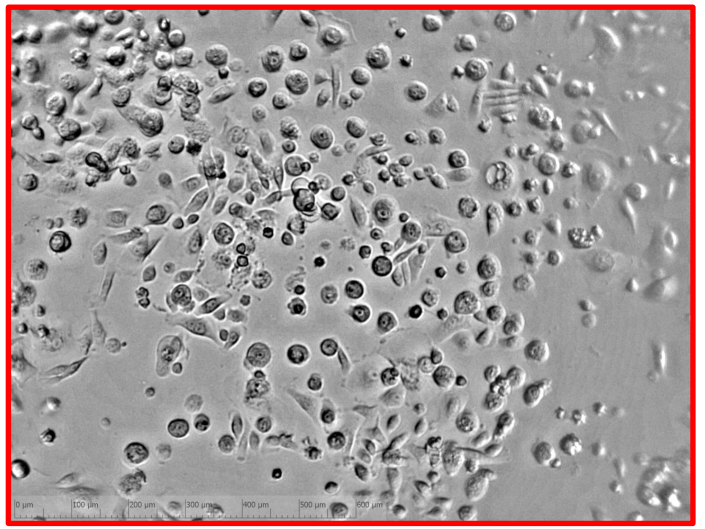

VideoA

Epithelix hAECM

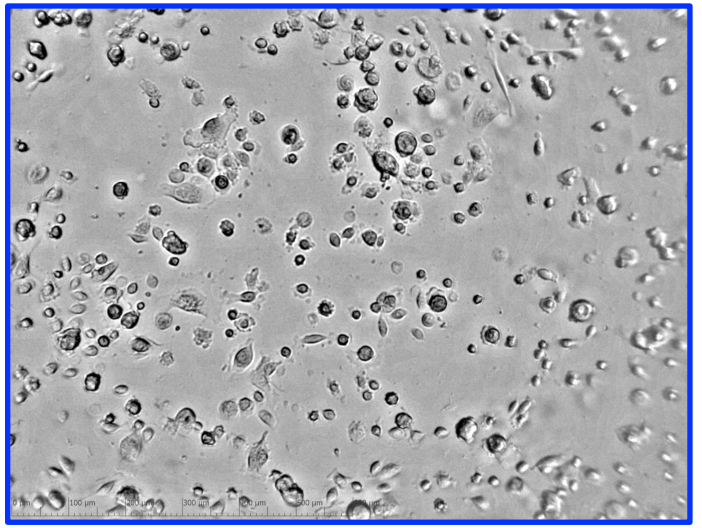

VideoB

Supplementary Figure 1. Surface area coverage and proliferation of BECs cultured in two different AEC growth medium over time (using the zenCELL owl incubator microscope (LabLogic, UK)). **A** Error bars represent mean ± SEM of *N* = 3 independent experiments. **B** Representative timelapse videos 0-84 h of one region of interest.

Supplementary Figure 2

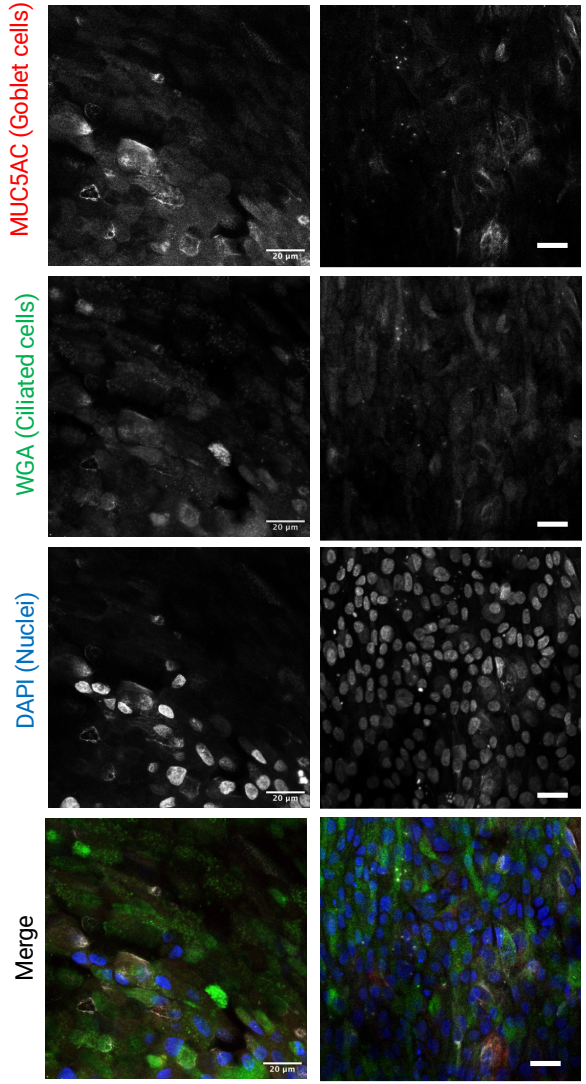

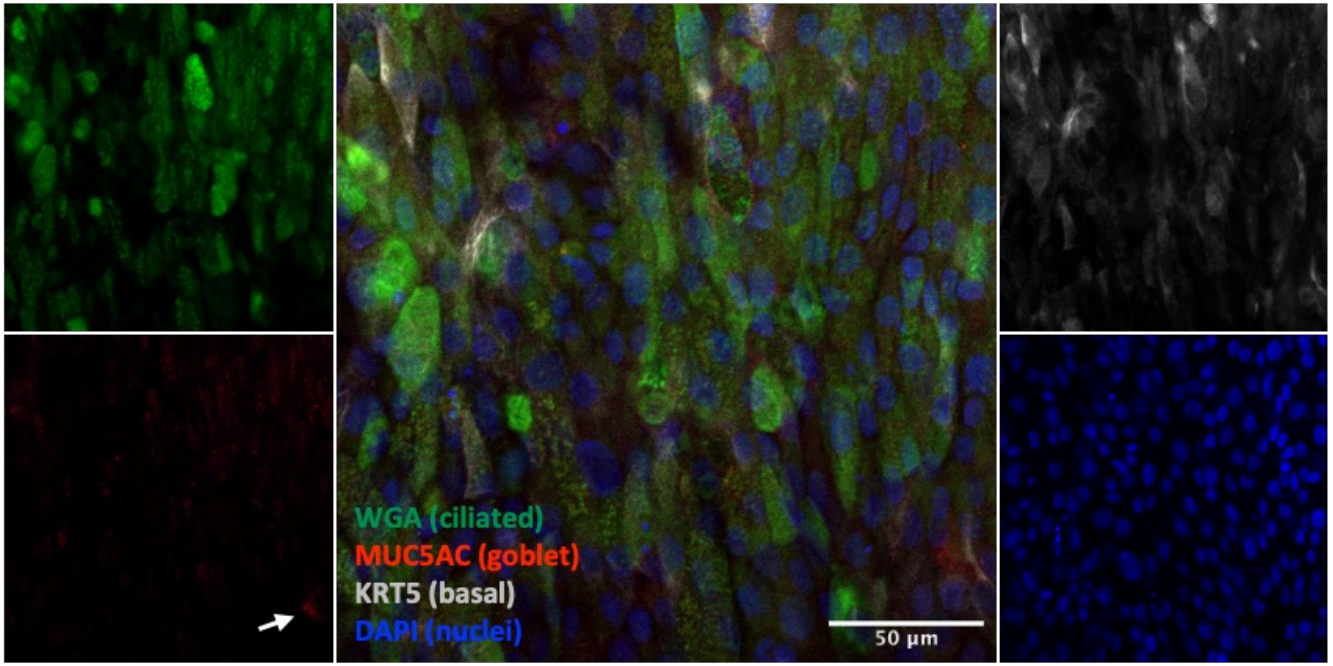

Supplementary Figure 2. Representative IF image to show expression of WGA (green, ciliated cell), MUC5AC (red, goblet cell) and KRT5 (grey, basal cell) staining. Nuclei (blue) counterstained with DAPI stained using animal-free reagents. Scale bars = 25µm (left) or 50µm (above).